) D. A. Evans, K. T. Chapman, E. M. Carreira, *J. Am. Chem. Soc.* **1988**, *110*, 3560.

[5] Y. Q. Tu, L. D. Sun, P. Z. Wang, *J. Org. Chem.* **1999**, *64*, 629.

[6] To the best of our knowledge, only a few SmI$_2$-promoted reactions are catalytically effective. See a) J. L. Namy, J. Souppe, J. Collin, H. B. Kagan, *J. Org. Chem.* **1984**, *49*, 2045; b) J. Prandi, J. L. Namy, G. Menoret, H. B. Kagan, *J. Organomet. Chem.* **1985**, *285*, 449; c) J. Collin, J. L. Namy, H. B. Kagan, *New J. Chem.* **1986**, *10*, 229; d) X. Lu, S. Ma, J. Zhu, *Tetrahedron Lett.* **1988**, *29*, 5129; e) D. A. Evans, A. H. Hoveyda, *J. Am. Chem. Soc.* **1990**, *112*, 6447; f) D. A. Evans, D. L. Rieger, T. K. Jones, S. W. Kaldor, *J. Org. Chem.* **1990**, *55*, 6260; g) P. V. Weghe, J. Collin, *Tetrahedron Lett.* **1993**, *34*, 3881; h) N. Takayuki, S. Hiroyuki, S. Satoshi, I. Yasutaka, *Tetrahedron Lett.* **2000**, *41*, 3389.

[7] For Tishchenko reactions, see: a) K. Yokoo, N. Mine, H. Taniguchi, Y. Fujiwara, *J. Organomet. Chem.* **1985**, *279*, C19; b) E. R. Burkhardt, R. G. Bergman, C. H. Heathcock, *Organometallics* **1990**, *9*, 30; c) S.-Y. Onozawa, T. Sakakura, M. Tanaka, M. Shiro, *Tetrahedron* **1996**, *52*, 4291; d) T.-H. Chuang, J.-M. Fang, W.-T. Jiaang, Y.-M. Tsai, *J. Org. Chem.* **1996**, *61*, 1794; e) R. Mahrwald, B. Costisella, *Synthesis* **1996**, 1087; f) Y. Umekawa, S. Sakaguchi, Y. Nishiyama, Y. Ishii, *J. Org. Chem.* **1997**, *62*, 3409; g) L. Lu, H.-Y. Chang, J.-M. Fang, *J. Org. Chem.* **1999**, *64*, 843; h) M. Adinolfi, G. Barone, F. De Lorenzo, A. Iadonisi, *Synlett* **1999**, 336; i) T. Ooi, T. Miura, K. Takaya, K. Maruoka, *Tetrahedron Lett.* **1999**, *40*, 7695; j) C. Delas, O. Blacque, C. Moïsoe, *J. Chem. Soc. Perkin Trans. 1* **2000**, 2265; k) C. M. Mascarenhas, S. P. Miller, P. S. White, J. P. Morken, *Angew. Chem.* **2001**, *113*, 621; *Angew. Chem. Int. Ed.* **2001**, *40*, 601.

[8] a) P. Girard, L. Namy, H. B. Kagan, *J. Am. Chem. Soc.* **1980**, *102*, 2693; b) H. B. Kagan, M. Sasaki, J. Collin, *Pure Appl. Chem.* **1988**, *60*, 1725; c) H. B. Kagan, *New J. Chem.* **1990**, *14*, 453; d) G. A. Molander, *Chem. Rev.* **1992**, *92*, 29; e) G. A. Molander, C. R. Harris, *Chem. Rev.* **1996**, *96*, 307; f) M. Kawatsura, E. Kishi, M. Kito, T. Sakai, H. Shirahama, F. Matsuda, *Synlett* **1997**, 497; g) A. Krief, A.-M. Laval, *Chem. Rev.* **1999**, *99*, 745; h) C. U. Dinesh, H.-U. Reissig, *Angew. Chem.* **1999**, *111*, 874; *Angew. Chem. Int. Ed.* **1999**, *38*, 789; i) N. Taniguchi, T. Hata, M. Uemura, *Angew. Chem.* **1999**, *111*, 1311; *Angew. Chem. Int. Ed.* **1999**, *38*, 1232; j) K. Ohmori, M. Kitamura, K. Suzuki, *Angew. Chem.* **1999**, *111*, 1304; *Angew. Chem. Int. Ed.* **1999**, *38*, 1226; k) J. Concellón, P. L. Bernad, J. A. Pérez-Andrés, *Angew. Chem.* **1999**, *111*, 2528; *Angew. Chem. Int. Ed.* **1999**, *38*, 2384; l) G. E. Keck, C. A. Wager, T. Sell, T. T. Wager, *J. Org. Chem.* **1999**, *64*, 2172; m) J. M. Aurrecoechea, R. Fañanás, M. Arrate, J. M. Gorgojo, N. Aurrekoetxea, *J. Org. Chem.* **1999**, *64*, 1893; n) T. Kikukawa, T. Hanamoto, J. Inanaga, *Tetrahedron Lett.* **1999**, *40*, 7497; o) L. Yet, *Chem. Rev.* **2000**, *100*, 2963; p) T. Kan, S. Nara, T. Ozawa, H. Shirahama, F. Matsuda, *Angew. Chem.* **2000**, *112*, 363; *Angew. Chem. Int. Ed.* **2000**, *39*, 355; q) S. M. Kim, I. S. Byun, Y. H. Kim, *Angew. Chem.* **2000**, *112*, 744; *Angew. Chem. Int. Ed.* **2000**, *39*, 728; r) X. Jiang, C. Wang, Y. Hu, H. Hu, *J. Org. Chem.* **2000**, *65*, 3555; s) A. Caracoti, R. A. Flowers, *Tetrahedron Lett.* **2000**, *41*, 3039.

[9] E. D. Mihelich, *Tetrahedron Lett.* **1979**, *20*, 4729.

[10] K. Mashimo, Y. Sato, *Tetrahedron* **1970**, *26*, 803.

[11] a) J. Souppe, L. Danon, J. L. Namy, H. B. Kagan, *J. Organomet. Chem.* **1983**, *250*, 227; b) J. Souppe, J. L. Namy, H. B. Kagan, *Tetrahedron Lett.* **1983**, *24*, 765.

[12] *n*BuLi (1 M, 2 equiv) was added to a solution of 1,2-diphenyl-1,2-ethanediol (1 equiv) in dry THF under Ar at 0°C, and the reaction mixture stirred for 0.5 h. The reaction mixture (dilithium 1,2-diphenylethanediolate) was then added to a suspension of SmI$_3$ (2 equiv) in dry THF by syringe and stirred for 1 h at RT under Ar. The product thus formed (see Scheme 2) was used in the reaction as catalyst, and the result was similar to that obtained in the general procedure. For a similar experimental procedure, see: D. A. Evans, S. G. Nelson, M. R. Gagné, A. R. Muci, *J. Am. Chem. Soc.* **1993**, *115*, 9800.

[13] T. Imamoto, M. Ono, *Chem. Lett.* **1987**, 501.

[14] J. D. Wuest, *Acc. Chem. Res.* **1999**, *32*, 81.

Grafted Metal Oxide/Polymer/Carbon Nanostructures Exhibiting Fast Transport Properties**

Huan Huang and Linda F. Nazar*

Rechargeable lithium batteries are a superior alternative energy source for a variety of applications that demand advanced energy-storage systems.[1] However, accessing high charge/discharge rates without losing capacity is one of the biggest challenges, due to the often sluggish kinetics of Li$^+$ ion transport in solid electrodes.[2] Many otherwise suitable intercalation materials do not meet the criterion of fast ion and/or electron transport. In contrast to attempting to tailor a single material, nanocomposites can provide an optimum way of crafting desired characteristics for a target application.[3] Here, we describe a new class of materials which were prepared by the grafting of polymer electrolyte chains and metal oxide layers onto the surface of electronically conductive "graphite-like" carbon spheres. They exhibit an enhanced electrochemical response at remarkably high rates and improved electrochemical stability owing to their unique nanostructure.

A "nanostructure" containing two or more materials mixed on a nanometer scale, ideally is a composite in which the sum of the parts is greater than the whole. This concept, of fundamental interest for many years, is widely applicable.[4] Electrochemical applications include those involving V$_2$O$_5$, a widely studied cathode material that has kinetic limitations both for ionic and electronic transport.[5] Layered polymer/metal oxide nanocomposites of xerogel – V$_2$O$_5$[6] have shown tenfold enhancement of the Li$^+$ diffusion coefficient, owing to polymer "propping" of the host layers.[7] Layered nanocomposites of clays and polyethylene oxide produce highly ionically conductive materials potentially suitable for solid electrolyte applications.[8] Another approach has been to shorten the diffusion path. High surface area aerogel forms of V$_2$O$_5$ display a high capacity under pseudo-equilibrium conditions in thin films.[9] V$_2$O$_5$ prepared by electrodeposition in the presence of surfactants displays a porous thin-wall structure, also resulting in good behavior with a capacity of 220 mA h g^{-1} at a fast rate.[10, 11] Nonetheless, a potential drawback with high surface area materials is poor volumetric capacity, and the attendant increase in catalytically active surface sites if the sites are not blocked, ultimately resulting in electrolyte degradation. However, none of the above approaches gives rise to a readily prepared, nor stable electrochemical system, nor takes advantage of a chemically nanostructured design.

---

[*] Prof. L. F. Nazar, H. Huang
Department of Chemistry
and the Waterloo Centre for Materials Research
University of Waterloo
Waterloo, ON, N2L 3G1 (Canada)
Fax: (+1) 519-746-0435
E-mail: lfnazar@uwaterloo.ca

[**] This work was supported by the National Sciences and Engineering Council of Canada through a Research Grant to L.F.N. H.H. thanks the Link Foundation (USA) for a scholarship in 2001.

Supporting information for this article is available on the WWW under http://www.angewandte.com or from the author.

Here, we have prepared nanocomposites by chemically wiring both polyelectrolytes and the active metal oxide (V_2O_5) onto the surface of semigraphitic carbon black nanoparticles that serve as an electronically conductive core. Although V_2O_5 serves to illustrate the concept, the method is also applicable to other materials. Importantly, as the polymer-functionalized carbon is readily dispersed ("soluble") in polar solvents, the conductive particles can also be used to impregnate the interstices of insulating or poorly conductive high surface area materials with accessible micropores.

Our procedure for coating active materials on polymer electrolyte-grafted carbon black is illustrated in Scheme 1. We chose acetylene black as the core carbon support, because of its well-known electronic conductivity and small particle size (average diameter ~44 nm). Polyethylene glycol (PEG) with a molecular weight of 4600 (corresponding to a stretched chain length of ~28 nm) was grafted onto carbon particles that were surface-treated to produce carboxylic functional groups to anchor the PEG chains.[12, 13] The polyelectrolyte-functionalized carbon or C-PEG was coated with an aqueous dispersion of V_2O_5 lamellae ("sol"),[14] and dried at 140 °C to yield V_2O_5/C-PEG.

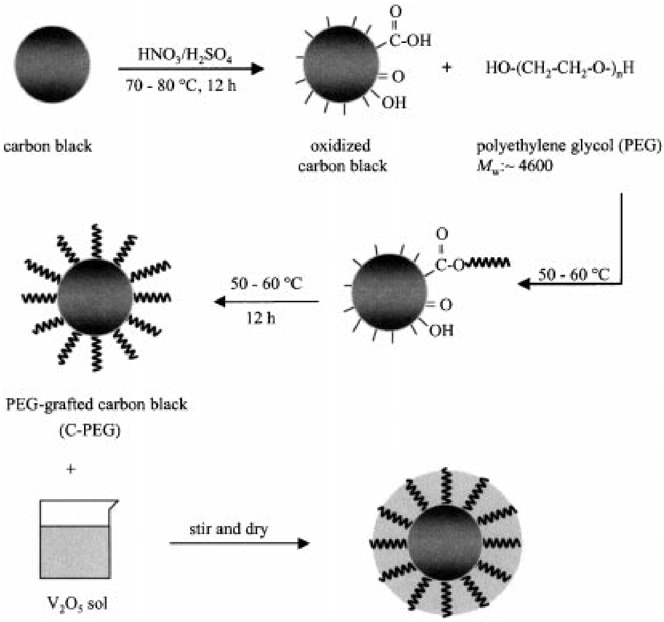

Scheme 1. The process for coating V_2O_5 xerogel on PEG-grafted carbon black.

The X-ray diffraction (XRD) pattern is representative of a lamellar material with an interlayer distance of 12.8 – 13.2 Å, which is greater than the value of anhydrous V_2O_5 (8.7 Å). The interlayer expansion of 4.1 – 4.5 Å indicates the PEG is intercalated between many of the V_2O_5 sheets, as a single layer in a stretched chain conformation, as seen in PEO/V_2O_5 nanocomposites. The increased interlayer spacing favors the Li^+ ion insertion process. IR spectroscopy suggests that the intercalated PEG also shows some structural modifications relative to PEG grafted on carbon (Figure 1). These small but significant changes[15] are due to steric interactions between the confined polymer and the framework and suggest subtle conformational differences between the incorporated and bulk forms of PEG. For electrochemical comparisons, V_2O_5 was also coated from the sol directly onto the carbon black, without functionalizing the surface with polyelectrolyte: these materials are referred to as V_2O_5/C. All compositions were determined by standard analysis methods.[16]

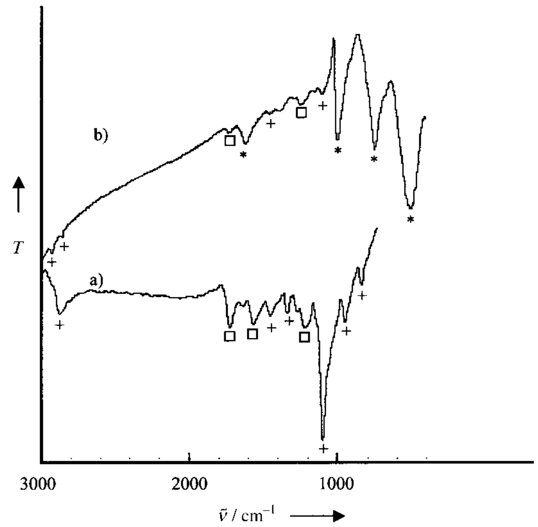

Figure 1. FT-IR spectra of a) C-PEG; b) V_2O_5/C-PEG nanoparticles. Band assignments: (+) = PEG; (*) = V_2O_5; □ = carbon.

Atomic force microscopy (AFM) images of the C-PEG and V_2O_5/C-PEG reveal that almost complete dispersion of the carbon particles can be achieved by grafting polyelectrolytes on their surface (Figure 2). The image of V_2O_5/C-PEG (Figure 2 a) shows an grouping of well-separated gum-drop-shaped particles on the mica surface with a mean diameter of about 85 nm, consisting of the carbon core (~44 nm) with a polyelectrolyte/metal oxide coating of about 40 nm. The image of the C-PEG particles (Figure 2 b) shows the particles have a size similar to V_2O_5/C-PEG, but with a different appearance of sharp furrows that suggests polymer "feathering" on the carbon surface. No distinct features are visible for the oxidized, but unfunctionalized carbon particles cast on the mica surface using the same procedure (Figure 2 c).

The electrochemical response of the hybrid nanostructured material over a wide range of current densities—measured by standard electrochemical methods and after thorough drying of the material—is greatly enhanced compared to that of a standard xerogel composite electrode (Figure 3). All experiments were performed under the same conditions with a current density of $10\,mA\,g^{-1}$ and a voltage window of 3.8 – 1.8 V versus Li. Data on the V_2O_5 xerogel are comparable to results previously reported. Whereas less than theoretical capacity is observed for the xerogel (1.3 Li/V_2O_5) and some irreversibility (Figure 3 a), for V_2O_5/C-PEG compositions almost complete reversibility is achieved, along with significantly reduced hysteresis and an almost doubled capacity (2.25 Li/V_2O_5 or $320\,mA\,h\,g^{-1}$; Figure 3 c). These improvements are attributed to a short diffusion distance for Li^+ and an increase of electronic contact upon employing this hybrid nanostructure. Note that better response vis a vis the xerogel

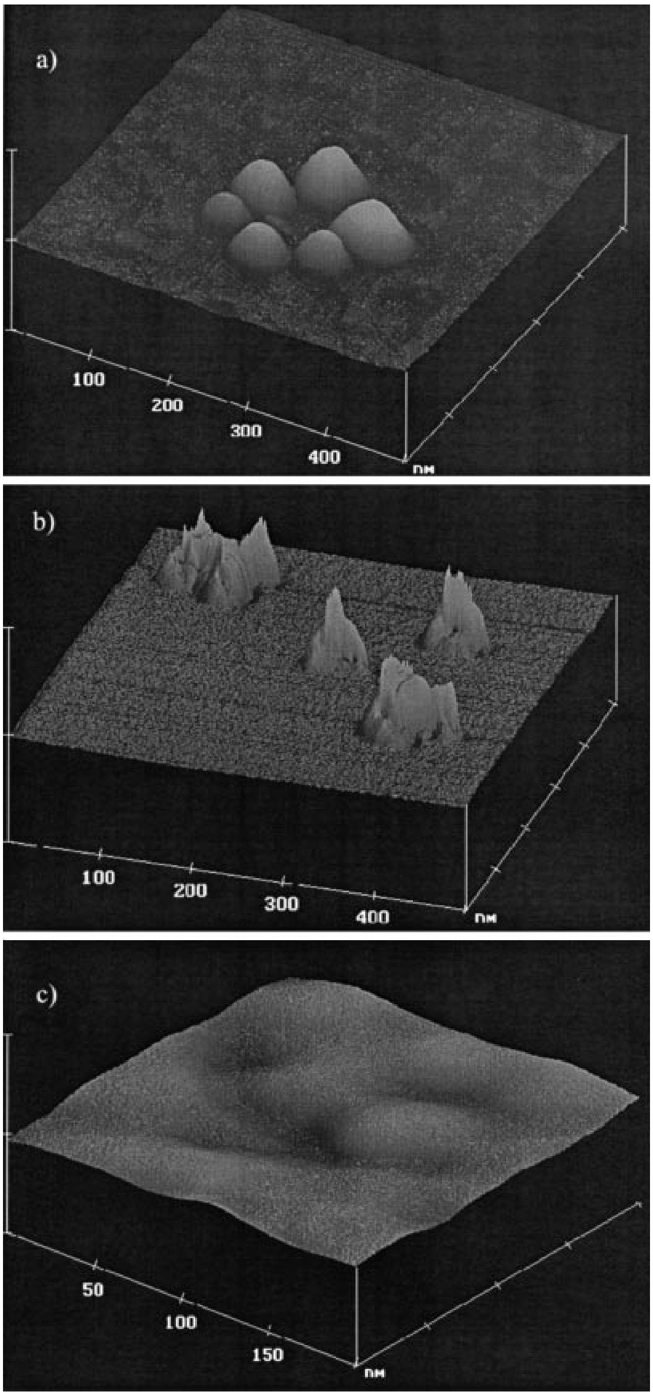

Figure 2. AFM images of a) V_2O_5/C-PEG nanoparticles on a mica surface; b) C-PEG; c) acid-functionalized carbon particles.

is also seen for the V_2O_5 directly coated on the carbon black particle (V_2O_5/C; Figure 3 b), but it is not as significant as with the polyelectrolyte present.

That there is rapid ion and electron transport in the hybrid nanostructured material is confirmed by varying the applied current (both for charging and discharging) to probe the comparative kinetic response. The effect of current density on working capacity on the three materials, up to current rates as high as 2000 mA g^{-1} (corresponding to a discharge rate of 14 C; that is, discharge or charge in 1/14 or 0.07 h) are summarized in Table 1. The capacity of the V_2O_5 xerogel decreased rapidly when a higher current was applied. At a current of 10 mA g^{-1}, the reversible capacity for the V_2O_5 xerogel was 160 mA h g^{-1}; increasing the current to 500 mA g^{-1} (~3.5 C) curtailed the available capacity to only about 30 mA h g^{-1}, which is less than 20 % of the initial value at the lower rate. This poor kinetic response is typical of a combination of electronic and ionic factors that limit redox accessibility under rapid rate conditions. Some improvement in the kinetic response is seen with V_2O_5/C as a result of the intimate contact of the oxide with the carbon. For the novel nanostructured composite, however, the rate capability was greatly improved. V_2O_5/C-PEG sustained current densities as high as 200 fold greater than the xerogel while maintaining an

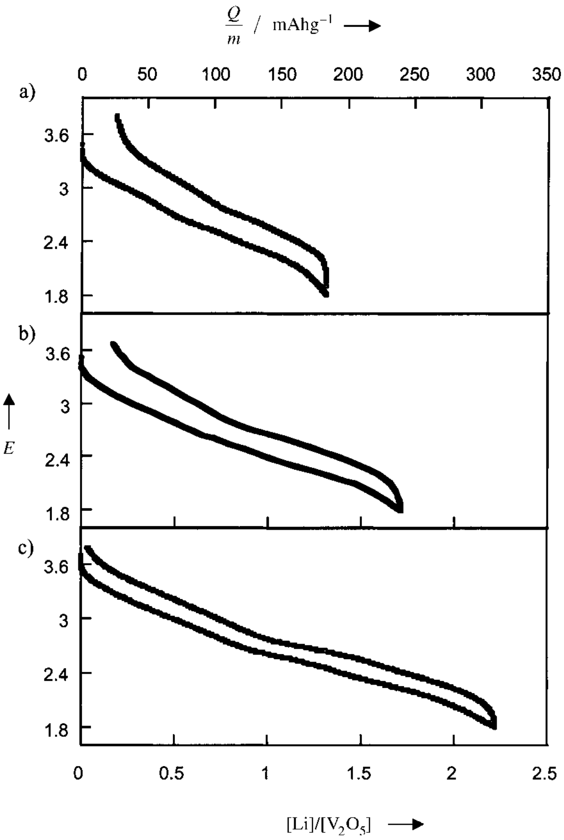

Figure 3. The first discharge–charge sweep for a) V_2O_5 xerogel, b) V_2O_5/C, and c) V_2O_5/C-PEG. Potential range: 3.8–1.8 V.

Table 1. Specific capacities of V_2O_5, V_2O_5/C, and V_2O_5/C-PEG at different current densities.

Current density [mA g^{-1}]	V_2O_5 xerogel specific capacity [mA h g^{-1}]	[%]	V_2O_5/C specific capacity [mA h g^{-1}]	[%]	V_2O_5/C-PEG specific capacity [mA h g^{-1}]	[%]
10	159	100	242	100	318	100
20	143	90	237	98	314	99
50	118	76	219	91	299	94
100	95	60	205	85	289	91
200	62	39	191	79	278	88
500	30	19	159	66	248	78
1000			115	48	224	71
2000					191	60

even higher capacity than the initial capacity of V_2O_5 gel at a low rate. At extremely high current densities of 1000 and 2000 mA g^{-1} (14 C), capacities of 225 and 190 mA h g^{-1}, respectively, were obtained for V_2O_5/C-PEG that correspond to about 71 % and 60 % of the capacity at a low current density. Based on its excellent kinetic response, this new nanostructured composite is very suitable for high current/power applications. This is summarized in the plot of specific power versus specific energy (Figure 4). The curve for the xerogel levels off at high power, indicating that the available energy becomes less. V_2O_5/C-PEG exhibits much better high power output capability. Even at 5000 W kg^{-1}, 70 % of the specific energy is still available.

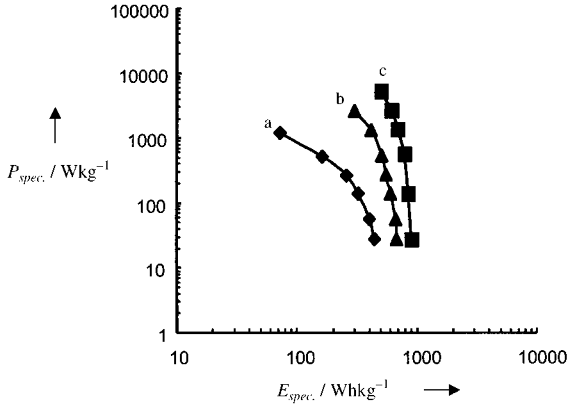

Figure 4. Power (P) – energy (E) plots of a) V_2O_5 xerogel, b) V_2O_5/C, and c) V_2O_5/C-PEG that illustrate the rate response.

The comparison in Figure 5 with the other composite materials indicates that the hybrid nanostructured material has not only substantially higher sustainable capacities, but also better long-term stability. Note the almost complete reversibility does not lead to a drop in capacity in the initial few cycles, whereas the other two materials display a—relatively common—initial decrease in capacity. This behavior is usually ascribed to irreversible reaction of lithium with surface defects, or entrapment in the structure, which clearly does not occur in the nanostructure.

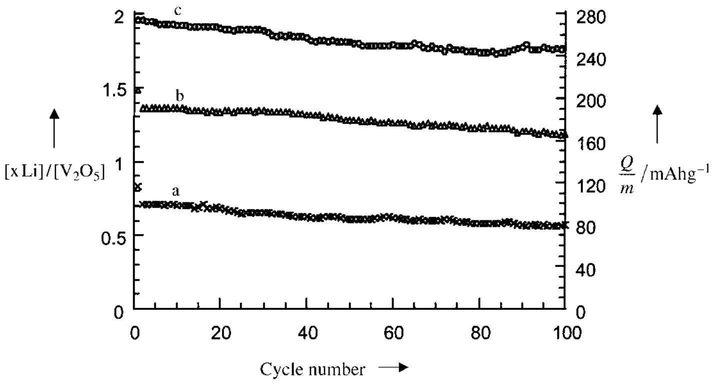

Figure 5. Capacity retention on cycling for a) V_2O_5 xerogel, b) V_2O_5/C, and c) V_2O_5/C-PEG. Current density: 100 mA g^{-1}; potential range: 3.8 – 1.8 V.

The grafted nanostructured materials we report here can be classified as fast transport materials on the basis of their kinetic response to high current densities. It is likely that the observed behavior is the result of the material being a multiphase composite; thus all factors (facile Li^+ transport owing to the polyelectrolyte component; electron transport due to the wiring of the V_2O_5 component to the conductive carbon surface, and the short diffusive path length) contribute. The advantages of such nanostructured materials arising from this combination are also synergistic: the mechanical strength of this composite is reinforced by the polymer chains, and the unique hybrid structure allows a contiguous V_2O_5 phase to bridge the gap between adjacent carbon particles, thus suppressing detrimental grain boundary effects. Experiments in progress will determine the relative contribution of these factors to the overall properties.

Experimental Section

Carbon black was treated with concentrated HNO_3/H_2SO_4 (1:1 v/v) at 70 – 80 °C for 12 h, and then washed with deionized water, and dried at 80 °C in an oven before use. Dispersal of 20 mg of this acid-treated carbon black in 100 mL H_2O gave a pH value of about 3.1, indicating that acidic groups were formed on the carbon surface. Confirmation was provided by the appearance of a new band in the IR spectrum at 1716 cm^{-1}, characteristic of the carboxylic group. The acid-oxidized carbon black was dispersed in deionized water and mixed with PEG solution with the desired weight ratio of carbon and polymer. The solution was heated and stirred at 50 – 60 °C for 12 h, and dried to give PEG-grafted carbon black (C-PEG). C-PEG is readily dispersed in water to form a completely stable non-settling suspension. IR spectra of C-PEG revealed that the grafting process led to broader bands of PEG compared to those of pure PEG, shifting the C=O and C–O bands of carbon black from 1716 and 1588 to 1736 and 1557 cm^{-1}, respectively, and producing a new band at 1643 cm^{-1}.

To form the V_2O_5 coating, V_2O_5 xerogel was dried to prepare free-standing films ($V_2O_5 \cdot x H_2O$, x: 1.6 – 1.8 depending on humidity), that displayed a typical lamellar structure with an interlayer distance d of 11.5 Å. The exact water content of the V_2O_5 xerogel film was determined by thermal analysis; the solid was then ground into powder and dissolved in water with the aid of ultrasound to obtain a clear dark red V_2O_5 sol, which was then mixed with well-dispersed C-PEG in different weight ratios.

Characterization: AFM was performed using a Digital Instruments NanoScope Scanning Probe Microscope. Samples of C-PEG and V_2O_5/C-PEG for AFM were prepared by dispersing the material in methanol using ultrasound for 10 min, and then depositing the suspension onto mica and drying it at 60 °C for 2 h.

Working electrodes were prepared from the nanocomposite, acetylene black, and polyvinylidene fluoride (PVDF) with a weight ratio of 85 %, 10 %, and 5 %, respectively, as previously reported,[7] with a loading of the active material of 3 – 4 mg. After evaporation of the solvent, all the electrodes were heated at 140 °C for at least 2 h prior to cell assembly to remove bound water. Swagelok-type cells were assembled in an argon-filled glove box and studied uder galvanostatic condition between voltage limits using a MacPile system. All potentials were controlled and recorded relative to a Li metal electrode.

Received: May 21, 2001 [Z17155]

---

[1] M. Armand, *Volta Award Address, 10th International Meeting on Lithium Batteries, Electrochemical Society* (Lake Como Italy) **2000**, Abstract 26; D. Aurbach, E. Zinigrad, H. Teller, P. Dan, *J. Electrochem. Soc.* **2000**, *147*, 1274.
[2] R. J. Brodd, *Electrochem. Soc. Interface* **1999**, *8(3)*, 20.
[3] P. Calvert, *Nature* **1999**, *399*, 210, and references therein.

[4] a) *Hybrid Organic-Inorganic Composites, Vol. 585* (Eds.: J. E. Mark, C. Y-C. Lee, P. A. Bianconi), American Chemical Society, Washington, DC, **1995**; b) special issue on nanostructured materials; *Chem. Mater.* **1996**, *8(8)*, and references therein; c) R. Gangopadhyay, A. De, *Chem. Mater.* **2000**, *12*, 608; d) K. G. Sharp, *Adv. Mater.* **1998**, *10*, 1243; e) P. J. Hagrman, D. Hagrman, J. Zubieta, *Angew. Chem.* **1999**, *111*, 2798; *Angew. Chem. Int. Ed.* **1999**, *38*, 2638; f) B. E. Koene, L. F. Nazar, *Solid State Ionics Diffusion and Reactions* **1996**, *89(1–2)*, 147.

[5] a) E. Potiron, A. Le Gal La Salle, A. Verbaere, Y. Piffard, D. Guyomard, *Electrochim. Acta* **1999**, *45*, 197; b) E. Potiron, A. Le Gal La Salle, S. Sarciaux, Y. Piffard, D. Guyomard, *J. Power Sources* **1999**, *81*, 666.

[6] a) Y. J. Liu, D. C. DeGroot, J. L. Schindler, C. R. Kannewurf, M. G. Kanatzidis, *Chem. Mater.* **1992**, *3*, 992; b) Y. J. Liu, J. L. Schindler, D. C. DeGroot, C. R. Kannewurf, W. Hirpo, M. G. Kanatzidis, *Chem. Mater.* **1996**, *8*, 525.

[7] a) F. Leroux, G. R. Goward, W. P. Power, L. F. Nazar, *J. Electrochem. Soc.* **1997**, *144*, 886–3895; b) F. Leroux, B. E. Koene, L. F. Nazar, *J. Electrochem. Soc.* **1996**, *143*, L181–182.

[8] a) S. Wong, S. Vasudevan, R. A. Vaia, E. P. Giannelis, D. Zax, *J. Am. Chem. Soc.* **1995**, *117*, 7568; b) M. M. Doeff, J. S. Reed, *Solid State Ionics Diffusion and Reactions* **1998**, *113–115*, 109.

[9] a) K. Salloux, F. Chaput, H. P. Wong, B. Dunn, *J. Electrochem. Soc.* **1995**, *142*, L191; b) D. B. Le, S. Passerini, A. L. Tipton, B. B. Owens, W. H. Smyrl, *J. Electrochem. Soc.* **1995**, *142*, L102; c) F. Coustier, S. Passerini, W. H. Smyrl, *J. Electrochem. Soc.* **1998**, *145*, L73; d) F. Coustier, J.-M. Lee, S. Passerini, W. H. Smyrl, *Solid State Ionics* **1999**, *116*, 279.

[10] P. Liu, J-G. Zhang, C. E. Tracy, J. A. Turner, *Electrochem. Solid-State Lett.* **2000**, *3*, 163.

[11] Data obtained in a voltage window of 4–1.5 V, with only 1 mg cm^{-2} of active material in the film, at a rate of 5 C. The latter refers to discharge or charge of 1 Li in 1/5 of an hour.

[12] a) Y. Choquette, M. Gauthier, C. Michot, M. Armand, Canadian Patent CA2248304 **1998**; b) N. Tsubokawa, *Prog. Polym. Sci.* **1992**, *17*, 417; c) J.-H. Lin, H.-W. Chen, K.-T. Wang, F.-H. Liaw, *J. Mater. Chem.* **1998**, *8*, 2169.

[13] *Carbon black: science and technology* (Eds.: J.-B. Donnet, R. C. Bansal, M.-J. Wang), Marcel Dekker, New York, **1993**.

[14] J. Lemerle, L. Nejem, J. Lefebvre, *J. Chem. Res.* **1978**, 5301; J. Livage, *Chem. Mater.* **1991**, *3*, 578.

[15] IR spectra of V_2O_5/C-PEG products showed three strong vibrations at 1000, 760, and 521 cm^{-1}, identical to those of V_2O_5 xerogel. In the CH_2 stretching absorption region, the strong band at 2877 cm^{-1} observed in bulk PEG is split into two bands at 2924 and 2854 cm^{-1}. In the region 1500–1000 cm^{-1}, no significant energy shifts were observed with respect to bulk PEG, but the relative intensities of the absorption bands were different and the band shapes were broader. The XRD and IR results confirmed that PEG was inserted into the V_2O_5 layers, and the insertion did not affect the structural integrity of the V_2O_5 framework.

[16] Chemical composition for *x*(Li) for all materials were calculated from the formula weight of the materials determined by thermogravimetric and chemical analyses [%]; for V_2O_5/C-PEG: V_2O_5: 72.5, C: 12.1, PEG: 6.03; for V_2O_5/C: V_2O_5: 72.1, C: 16.6.

Combined Effects of Metal and Ligand Capable of Accepting a Proton or Hydrogen Bond Catalyze Anti-Markovnikov Hydration of Terminal Alkynes**

Douglas B. Grotjahn,* Christopher D. Incarvito, and Arnold L. Rheingold

Metalloenzyme catalysts such as carboxypeptidase use the cooperative effects of a metal ion and suitably placed organic functional groups capable of proton transfer or hydrogen bonding.[1, 2] Using this cue from Nature, we are making complexes of general structure **A** (Scheme 1) where L is a ligating atom and N is part of a heterocycle, particularly imidazole. Our results clearly indicate that the combined effects of a metal and a proton or hydrogen bond acceptor as in **A** produce a binding pocket for a polar ligand. We report herein on the anti-Markovnikov hydration of terminal alkynes [Eq. (1)], which produces aldehydes, rather than the isomeric ketones, with selectivities of up to 1000 to 1.

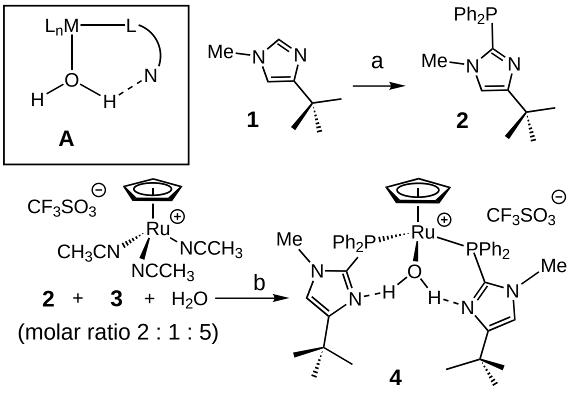

Scheme 1. Design (**A**) and synthesis of catalyst **4**. a) *n*BuLi, THF, −78 to −50 °C, 3 h, then ClPPh$_2$, warming to RT, 51 %; b) CDCl$_3$ or CH$_2$Cl$_2$, RT, <2 h, 98 %.

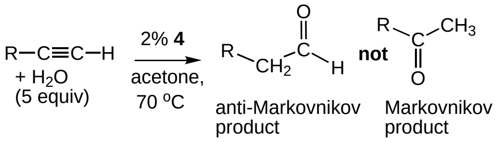

(1)

---

[*] Prof. D. B. Grotjahn
Department of Chemistry
San Diego State University
5500 Campanile Drive
San Diego, CA 92182-1030 (USA)
Fax: (+1) 619-594-4634
E-mail: grotjahn@chemistry.sdsu.edu

C. D. Incarvito, Prof. A. L. Rheingold
Department of Chemistry and Biochemistry
University of Delaware
Newark, DE 19716 (USA)

[**] The support of San Diego State University is acknowledged.

Supporting information for this article is available on the WWW under http://www.angewandte.com or from the author.